Available at www.sciencedirect.com

ScienceDirect

journal homepage: www.elsevier.com/locate/he

Load sharing using fuzzy logic control in a fuel cell/ultracapacitor hybrid vehicle

M.C. Kisacikoglu[a,*], M. Uzunoglu[a,b], M.S. Alam[a]

[a]Department of Electrical and Computer Engineering, University of South Alabama, 1508 Middle Drive, Mobile, AL 36688, USA
[b]Department of Electrical Engineering Yildiz Technical University, Istanbul 34349, Turkey

ARTICLE INFO

Article history:
Received 15 August 2008
Received in revised form
11 November 2008
Accepted 11 November 2008
Available online 30 December 2008

Keywords:
Fuel cell
Dc–dc converter
Ultracapacitors
Hybrid system
Fuzzy logic

ABSTRACT

Fuel cell (FC) and ultracapacitor (UC) based hybrid power systems appear to be very promising for satisfying high energy and high power requirements of vehicular applications. The improvement in control strategies enhances dynamic response of the FC/UC hybrid vehicular power system under various load conditions. In this study, FC system and UC bank supply power demand using a current-fed full bridge dc–dc converter and a bidirectional dc–dc converter, respectively. We focus on a novel fuzzy logic control algorithm integrated into the power conditioning unit (PCU) for the hybrid system. The control strategy is capable of determining the desired FC power and keeps the dc voltage around its nominal value by supplying propulsion power and recuperating braking energy. Simulation results obtained using MATLAB® & Simulink® and ADVISOR® are presented to verify the effectiveness of the proposed control algorithm.

1. Introduction

Increasing effects of global warming and depleting oil reserves has led researchers to develop alternative methods so as to meet high energy demand of transportation systems. The fuel cell technology is one of the systems used in vehicle applications for being an alternative energy converter (hydrogen to electric) and environmentally-friendly [1–3]. Coupled with this, almost all of the major companies have publicized ambitious plans to introduce hydrogen powered vehicles in the market. This vehicle type promises very clean operation and shows higher energy efficiency than conventional vehicles [4].

Fuel cells are electrochemical devices that convert the chemical energy of a reaction directly into electrical energy. Among the various types of fuel cells, PEMFC appears to be more attractive due to its simplicity, viability, quick start up, prompt response time, higher power density, long cycle life and operation at lower temperatures [5–8]. Therefore, PEMFC is a serious candidate for automotive applications [5]. However, a sole FC system may not be sufficient to satisfy the load demands, especially during peak power demand periods or transient events mostly seen in vehicular applications. Moreover, if the FC system alone supplies all power demand, it would increase the size and cost of the FC system as well as the hydrogen fuel consumption. Without an extra energy source, the FC system has to respond to transient and peak loads. Also, since the FC system cannot sink power, braking energy is not recycled. Hence, the overall fuel consumption increases in a stand alone FC system. As a result, using only the FC system becomes insufficient and cost prohibitive to meet the load profile for a vehicle. Therefore, the FC system should be supplemented with a less expensive power source with fast response characteristics.

* *Corresponding author*. Tel.: +1 865 974 9886; fax: +1 865 974 5483.
E-mail address: mkisacik@utk.edu (M.C. Kisacikoglu).
0360-3199/$ – see front matter © 2008 International Association for Hydrogen Energy. Published by Elsevier Ltd. All rights reserved.
doi:10.1016/j.ijhydene.2008.11.035

In most of today's hybrid applications, batteries are placed as energy storage systems. Recent studies research the feasibility of using battery along with fuel cell in vehicles as an assistant power source [8–11]. While batteries are expected to become a viable source to power coming generations of electric vehicles, ultracapacitors are also tested with different control methods to complement FCs [12,13]. UC is a better partner to FC than battery for several reasons. Firstly, due to the low power density of the battery it cannot release its charge fast enough when a transient occurs. Secondly, although batteries are considered to be the main energy storage device for future electric vehicles, their cycle and calendar life should still be improved. Lastly, batteries are more suited to supply steady load profile rather than giving the transient load power because of its internal dynamics. On the other hand, ultracapacitors promise to be a good alternative in vehicular applications. Ultracapacitors are electrical energy storage devices which offer significantly better energy densities than conventional capacitors, better power densities than conventional batteries, and can be constructed in modular and/or stackable format. The charge and discharge time of a UC varies from fractions of a second to several minutes, while providing maintenance-free operation. Ultracapacitors provide the lowest cost per Farad, have extremely high cycling capability, and are environmentally safe [14,15]. The capacitance of UCs may vary from a few Farads to several thousand Farads per cell [16]. Because of the aforementioned unique characteristics, UCs are utilized for a wide range of applications. Therefore, a UC bank can effectively serve as a cost effective alternative to batteries, especially during short peak demand periods.

UCs have high specific power density, and are suitable to operate in conjunction with fuel cells in hybrid electric vehicles. When coupled with an FC system, UC bank provides the sudden transient power demand during acceleration and hill climbing and alleviates the slow response problem of the FC system [17]. In addition, a UC can also be used to store excess power during regenerative braking. Therefore, by operating FC and UC in parallel, both steady-state and peak power demand can be satisfied. In other words, FC/UC hybrid system offers high energy output with high responsiveness and high storage capability [18]. Besides, in transient conditions, insufficient humidification with gas starvation or flooding problems may occur due to instant load changes. The proposed FC/UC hybrid system ensures that the membrane of the FC system is not subjected to transients and sharp peak loads, thus increasing the lifetime of the FC system [19].

Another significant contribution to effective operation is the design and control of the PCU integrated into the hybrid system. There are several PCU topologies that can be used in hybrid systems. The location of pulse power source and the connection strategy distinguish the topology of the PCU in a hybrid system. Among these topologies, parallel connection of the FC system and UC bank to the dc bus via two different dc–dc converters may be chosen for better system utilization [20,21].

In this paper, a current-fed full bridge dc–dc converter and a bi-directional dc–dc converter are employed for the power control of the FC/UC hybrid system. This topology boosts low voltages of the FC system and UC bank to higher values and electrically isolates the hybrid power sources from the load. It enables the control of the dc bus voltage and satisfies a higher maximal torque of the electrical machine at lower ultracapacitor voltages [20].

The entire control strategy of the PCU is developed using fuzzy logic algorithm. In the control system, the average power demand of the load bus is continuously measured and FC system is supposed to meet the base load profile which is peak-shaved and transient-free. On the other hand, the UC system supplies the entire peak load demand as well as capturing the braking energy. Fuzzy logic controller (FLC) assigns different power points for the FC system rather than giving several operation modes in which the FC system would supply constant power. At the same time, FLC observes the state of charge (SOC) of the UC bank and utilizes the FC system to supply power not only to load but also to the UC bank. Therefore, the UC bank remains ready to supply peak power and recuperate braking energy. Additionally, FLC engages the UC bank to control the voltage of the dc link in order to take or supply the power difference between the load and the FC system.

2. System description and methodology

2.1. Design and dynamic modeling of a PEMFC

The PEMFC model used in this paper is realized in MATLAB & Simulink. This model has been built using the relationship between output voltage and partial pressures of hydrogen, oxygen and water. Fig. 1 shows the detailed model of the PEMFC, which is then embedded into the SimPowerSystems of MATLAB as a controlled voltage source and integrated into the overall system. The FC system model parameters used to obtain this model are as follows:

B,C	Constants to simulate the activation over voltage in PEMFC system (A^{-1}) and (V)
E	Nernst instantaneous voltage (V)
E_0	Standard no load voltage (V)
F	Faraday's constant (C (kmol)$^{-1}$)
I_{FC}	FC system current (A)
K_{an}	Anode valve constant ($\sqrt{\text{kmol kg}}$(atm s)$^{-1}$)
K_{H_2}	Hydrogen valve molar constant (kmol (atm s)$^{-1}$)
K_{H_2O}	Water valve molar constant (kmol (atm s)$^{-1}$)
K_{O_2}	Oxygen valve molar constant (kmol (atm s)$^{-1}$)
K_r	Modeling constant (kmol (s A)$^{-1}$)
M_{H_2}	Molar mass of hydrogen (kg (kmol)$^{-1}$)
n_{H_2}	Number of hydrogen moles in the anode channel (kmol)
N_0	Number of series fuel cells in the stack
N_s	Number of fuel cell modules
p_{H_2}	Hydrogen partial pressure (atm)
p_{H_2O}	Water partial pressure (atm)
p_{O_2}	Oxygen partial pressure (atm)
q_{O_2}	Input molar flow of hydrogen (kmol (s)$^{-1}$)
$q_{H_2}^{in}$	Hydrogen input flow (kmol (s)$^{-1}$)

(continued)

$q_{H_2}^{out}$	Hydrogen output flow (kmol (s)$^{-1}$)
$q_{H_2}^{r}$	Hydrogen flow that reacts (kmol (s)$^{-1}$)
$q_{H_2}^{req}$	Amount of hydrogen flow required to meet the load change (kmol (s)$^{-1}$)
R	Universal gas constant ((1 atm) (kmol K)$^{-1}$)
R^{int}	FC internal resistance (Ω)
RH–O	The hydrogen–oxygen flow ratio
T	Absolute temperature (K)
U	Utilization rate
V_{an}	Volume of the anode (m^3)
V_{cell}	Dc output voltage of FC system (V)
τ_{H_2}	Hydrogen time constant (s)
τ_{O_2}	Oxygen time constant (s)
τ_{H_2O}	Water time constant (s)
η_{act}	Activation over voltage (V)
η_{ohmic}	Ohmic over voltage (V)

The equation that relates molar flow of any gas (hydrogen) through the valve with its partial pressure inside the channel can be expressed as [22]

$$\frac{q_{H_2}}{p_{H_2}} = \frac{K_{an}}{\sqrt{M_{H_2}}} = K_{H_2}. \tag{1}$$

The ideal gas equation is applied to hydrogen,

$$p_{H_2} \cdot V_{an} = n_{H_2} \cdot R \cdot T. \tag{2}$$

From the Eq. (2) hydrogen pressure can be written as

$$p_{H_2} = \frac{R.T}{V_{an}} \cdot n_{H_2}. \tag{3}$$

Taking the derivative of the both sides of the above equation gives

$$\frac{d}{dt} p_{H_2} = \frac{R \cdot T}{V_{an}} \cdot \frac{d}{dt} n_{H_2} = \frac{R \cdot T}{V_{an}} \cdot q_{H_2} \tag{4}$$

The derivative of n_{H_2} is q_{H_2} which is hydrogen molar flow. There are three relevant contributions to the hydrogen molar flow; the input flow, the flow taking part in the reaction and the output flow. Therefore,

$$\frac{d}{dt} p_{H_2} = \frac{R \cdot T}{V_{an}} \cdot \left(q_{H_2}^{in} - q_{H_2}^{out} - q_{H_2}^{r} \right). \tag{5}$$

According to basic electrochemical relationships, the molar flow of hydrogen that reacts can be found as

$$q_{H_2}^{r} = \frac{N_0 \cdot I_{FC}}{2 \cdot F} = 2 \cdot K_r \cdot I_{FC}, \tag{6}$$

where

$$K_r = \frac{N_0}{4 \cdot F}. \tag{7}$$

Inserting Eq. (6) into Eq. (5) results the following equation:

$$\frac{d}{dt} p_{H_2} = \frac{R.T}{V_{an}} \cdot \left(q_{H_2}^{in} - q_{H_2}^{out} - 2 \cdot K_r \cdot I_{FC} \right). \tag{8}$$

Then, replacing output flow, $q_{H_2}^{out}$ with its definition in the Eq. (1) gives:

$$\frac{d}{dt} p_{H_2} = \frac{R.T}{V_{an}} \cdot \left(q_{H_2}^{in} - K_{H_2} \cdot p_{H_2} - 2 \cdot K_r \cdot I_{FC} \right). \tag{9}$$

Taking the Laplace transforms of both sides yields:

$$s \cdot p_{H_2}(s) - p_{H_2}(0) = \frac{R \cdot T}{V_{an}} \cdot \left(q_{H_2}^{in}(s) - K_{H_2} \cdot p_{H_2}(s) - 2 \cdot K_r \cdot I_{FC} \right), \tag{10}$$

where the initial condition of hydrogen partial pressure is zero. The following expression gives the hydrogen partial pressure as:

$$p_{H_2} = \frac{1/K_{H_2}}{1 + \tau_{H_2} s} \left(q_{H_2}^{in} - 2 \cdot K_r \cdot I_{FC} \right), \tag{11}$$

where

$$\tau_{H_2} = \frac{V_{an}}{K_{H_2} \cdot R \cdot T} \cdot s. \tag{12}$$

Similarly, water partial pressure and oxygen partial pressure can be obtained. The polarization curve for the PEMFC is obtained from the sum of the Nernst's voltage, the activation over voltage, and the ohmic over voltage. Assuming constant temperature and oxygen concentration, the FC output voltage may be expressed as [23–25]

$$V_{cell} = E + \eta_{act} + \eta_{ohmic}, \tag{13}$$

where

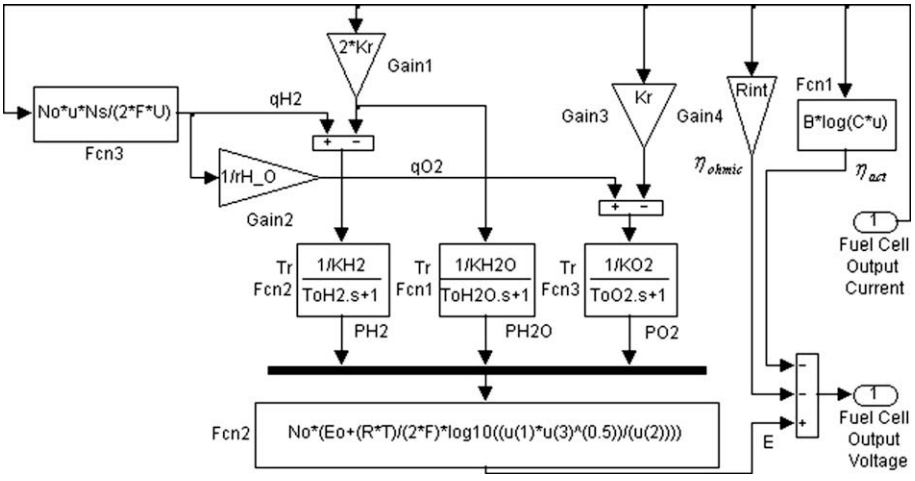

Fig. 1 – Dynamic model of the FC system.

$$\eta_{act} = -B\ln(CI_{FC}) \tag{14}$$

and

$$\eta_{ohmic} = -R^{int}I_{FC}. \tag{15}$$

Now, the Nernst's instantaneous voltage may be expressed as [23]

$$E = N_0\left[E_0 + \frac{RT}{2F}\log\left[\frac{p_{H_2}\sqrt{P_{O_2}}}{p_{H_2O}}\right]\right]. \tag{16}$$

The fuel cell system consumes hydrogen according to the power demand. The hydrogen is obtained from high-pressure hydrogen tank for stack operation. During operational conditions, to control hydrogen flow rate according to the FC power output, a feedback control strategy is utilized. To achieve this feedback control, FC current from the output is taken back to the input while converting the hydrogen into molar form [4,23]. The amount of hydrogen available from the hydrogen tank is given by

$$q_{H_2}^{req} = \frac{N_0 I_{FC}}{2\,FU}. \tag{17}$$

Depending on the FC system configuration, and the flow of hydrogen and oxygen, the FC system produces the dc output voltage. The hydrogen–oxygen flow ratio r_{H-O} in the FC system determines the oxygen flow rate [23]. Different time constants can be defined for fuel increase and fuel decrease [26].

2.2. Design and modeling of ultracapacitor bank

The classical equivalent circuit of the UC unit, shown in Fig. 2, consists of a capacitance (C), an equivalent series resistance (ESR) representing the charging and discharging resistance, and an equivalent parallel resistance (EPR) representing the self-discharging losses [4,27]. Since the EPR models leakage effects and influences long-term energy storage performance of the UC [28,29], only the ESR will be taken into account. Therefore, the voltage profile will depend on two components; a capacitive and a resistive component [30]. The UC bank model has been implemented in MATLAB and SimPowerSystems for this study.

2.3. Drive cycle

The urban dynamometer driving schedule (UDDS) [31] is selected as a reference cycle to model, design and simulate the proposed vehicle power system. Fig. 3 shows the power demand of a vehicle according to standard UDDS as a function

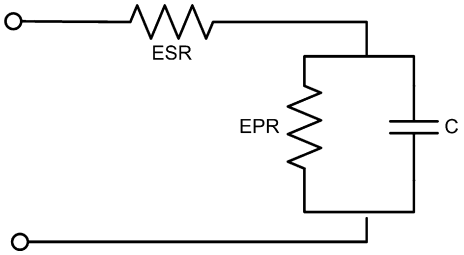

Fig. 2 – Classical equivalent model for the UC unit.

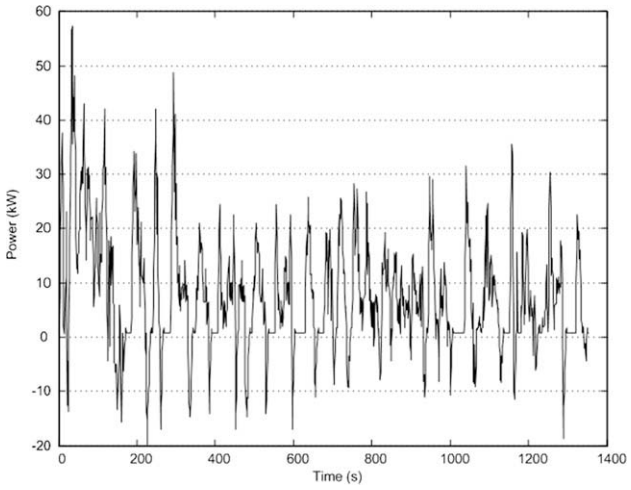

Fig. 3 – Power demand according to UDDS for an FC powered vehicle.

of time. Specific characteristics of the UDDS cycle are shown in Table 1.

The power demand required to meet the vehicle speed is obtained from the ADVISOR analysis tool and the load model is realized with respect to this power profile using the MATLAB and SimPowerSystems environment.

2.4. Power conditioning unit

Utilizing two different power sources simultaneously requires a power converter interface to effectively control the power flow. This power interface also allows sharing of the wheel power among the FC system and UC bank based on the rules defined in the fuzzy logic controller. The structure of the PCU is the same as the VW BORA Hy. Power [20] which consists of two different dc–dc converters – the first one used to connect the FC system and the second one to interface the UC bank. A current-fed full bridge dc–dc converter is employed to transfer the desired power from the FC system to the drive train. Not only the input voltage of the FC system is boosted to higher values, but also it is isolated from drive train with a high frequency transformer. Moreover, the FC system output current fluctuation is effectively reduced by using an input inductor [21]. Also, the switching sequence employed for the converter (duty ratio > 0.5) does not cause discontinuous operation on the current demanded from the FC system thus increasing the lifetime of the FC system.

Table 1 – Specific characteristics of UDDS drive cycle.

Time	1369 (s)
Distance	7.45 (miles)
Max. speed	56.7 (mph)
Avg. speed	19.6 (mph)
Max. accel.	1.48 (m $(s^2)^{-1}$)
Max. decel.	−1.48 (m $(s^2)^{-1}$)
Avg. accel.	0.51 (m $(s^2)^{-1}$)
Avg. decel.	0.58 (m $(s^2)^{-1}$)
Idle time	259 (s)

The UC bank transmits its power to the inverter through a bidirectional dc–dc converter. It functions as a current source full bridge converter when the UC bank is discharged and as a voltage source half bridge converter when the UC bank is charged [21]. The general system configuration is shown in Fig. 4.

2.5. *Fuzzy logic control*

The main requirements of the control algorithm are to satisfy the power demand and manage the power flow while ensuring efficient operation of the different power sources. The control system should utilize the FC system and UC bank to match the vehicle load profile by considering different features of the power sources. Since stable operation of the FC system is vital for efficiency, lifetime, and cost, the FC system should deliver the base load power without responding to peak power demand. Another purpose of the control system is to adopt the UC bank in stabilizing the dc link voltage. This enables power transfer to/from the UC bank and improves the overall driving performance [20].

The above mentioned requirements of the hybrid power system control were implemented using an FLC. The FLC relates the output values to inputs with 'IF…THEN' statements, called rules. It is especially suitable for processes with complex non-linear models. Unlike Boolean logic, which describes that a given input is either a member of a given set (logic 1) or not (logic 0), FLC solves problems that tend to change anywhere in the range of 0– 1 [43]. Therefore, the FLC offers smooth relocation of the output signal instead of sharp switching when one rule dominates the other.

The FLC has five inputs and three outputs as shown in Fig. 5. The first input is the difference between the average load current (ALC) and output current of the dc–dc converter of the FC system (I_{FC}) and the second one corresponds to the state of charge (SOC) of the UC bank. Using the data available from these two inputs, the FLC determines the FC system duty ratio (FCR), which corresponds to the first output. The FC system delivers power based on the decision of FLC and maintains a balance between delivering average load power and keeping SOC at its desired interval which is around 0.75. The UC bank should have enough charge to keep the voltage stable when the vehicle is accelerating and it should have enough space to recuperate energy during regeneration. The FC system supplies fundamental power by observing the SOC of the UC bank. The fundamental power corresponds to the average power if SOC is inside the desired interval. If SOC is higher than the expected value, the FC system delivers less power than the average in order to avoid overcharging the UC bank which may cause voltage increase in the dc bus. Similarly, if SOC is less than the expected value, then the FC system transfers more power. Thus, the UC bank is not discharged below 25% of the maximum energy storage capacity and the voltage does not fall below the desired value. In short, FC system delivers the base portion of the load and it is not disturbed by sudden peaks of the demand.

In the FLC, the Mac–Vicar Whelan rule base [44] is used. In order to ensure a better performance for the operation of the FC system, some modifications have been made when developing the FLC rules. The membership functions for the inputs and outputs are also shown in Fig. 5. The FLC utilizes the first two inputs and generates FCR as shown in Fig. 6. It is important to note that FCR does not fall below 0.5 and provides a continuous current path for the FC system.

Inputs 3 and 4 are the error voltage (voltage difference between desired voltage and bus voltage), V_{err} and its derivative, respectively. After the decision process, they transform into UC bank duty ratio for charging (UCR) and discharging (UDR), and ensure the stability of the dc bus voltage. Input 5, which is the transferred current to or from the UC bank, helps

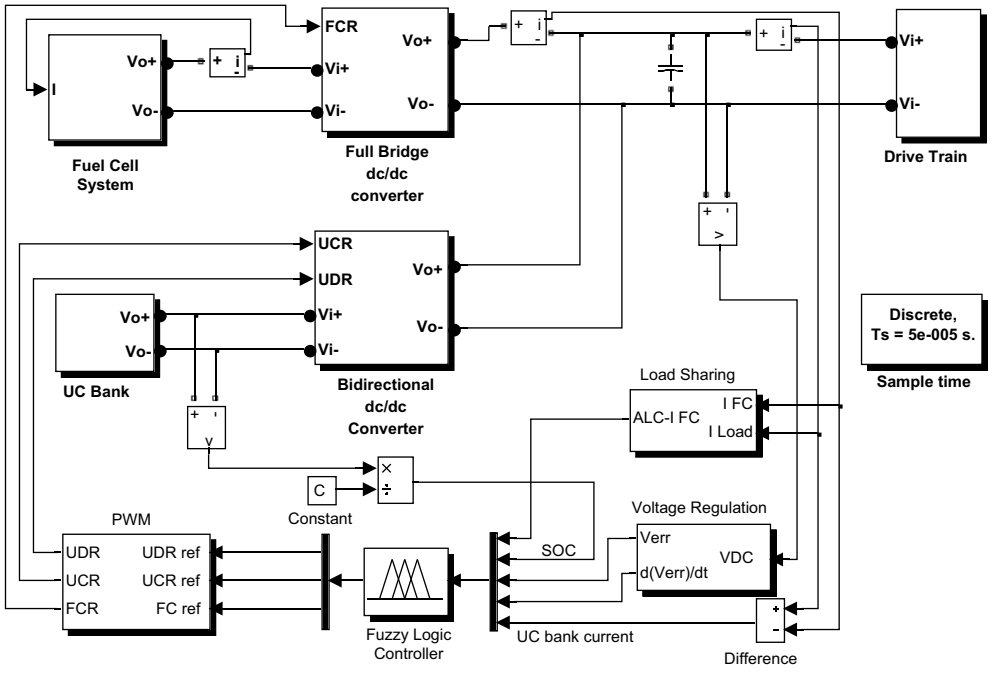

Fig. 4 – Hybrid system configuration.

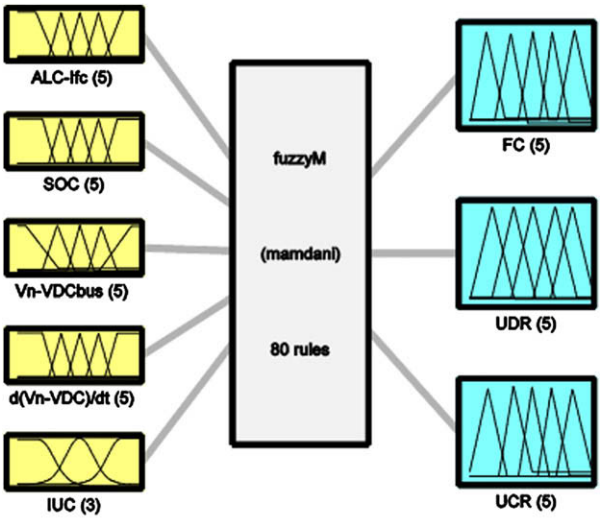

Fig. 5 – Fuzzy interference system.

the FLC to decide the exact time to start charging or discharging the UC bank. Also, at low UC bank currents, the FLC can employ both UDR and UCR in order to glide smoothly from charging to discharging, and vice versa. Therefore, the power difference between the load and FC system is transferred to or from the UC bank while keeping the voltage stable. The fuzzy inference system output surface for UDR and UCR is shown in Figs. 7 and 8, respectively.

The UCR and UDR complement each other and FLC calculates their final values based on the position of the UC bank current. If the UC bank charges or discharges with an absolute value greater than 13 A, then the UCR and UDR are calculated depending only on the 3rd and 4th inputs of the FLC. If it is on the verge of switching from charging to discharging or vice versa, where the UC bank current is less than the absolute value of 13A, the UCR and UDR generate outputs by observing the weight of the current states such as charge, neutral and discharge as illustrated in Fig. 9. Therefore, the system smoothly glides from one state to another.

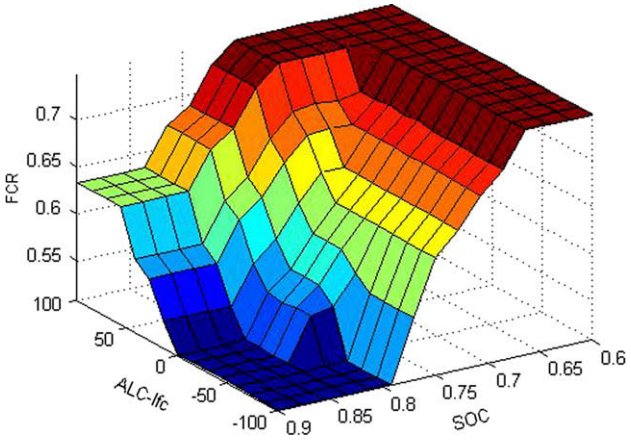

Fig. 6 – Fuzzy logic controller surface for FCR.

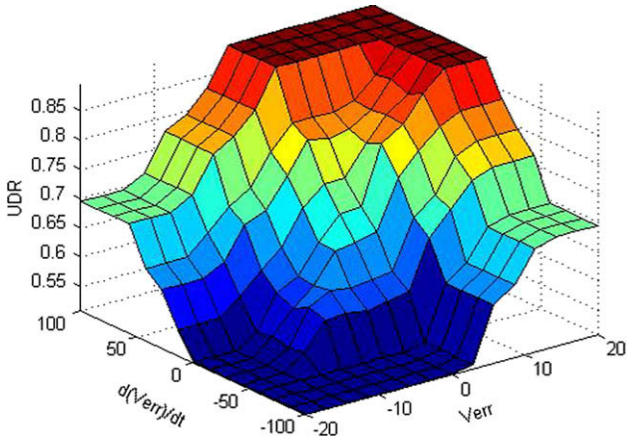

Fig. 7 – Fuzzy logic controller surface for UDR.

In order to better understand the rules used in FLC, FC system output power decision is given as an example in Table 2. The output power of the FC system is unidirectional and is always from the FC system to the load. FLC adjusts the duty ratio from NM to PM smoothly to give the necessary output power command. This command is decided using the battery SOC and the load power.

2.6. *Load sharing and sizing of the power sources*

To determine the appropriate sizes of the FC system and UC bank, it is essential to define the vehicle load sharing between these units. The FC system is sized to provide only the base load or cruising power of the vehicle, and the peak power for up-hill or accelerated driving is provided by the UC bank [5,17,32]. Mathematical definition of the base load can be defined as the average load power demanded by the drive train [33,34]. However, as it is seen from the first 300 s of the UDDS power profile shown in Fig. 10, UC bank would have to supply too much power while FC system is undersized with this load sharing algorithm. The proposed control algorithm uses the FC system as the primary power source and satisfies a stable power transfer from the FC system to the drive train.

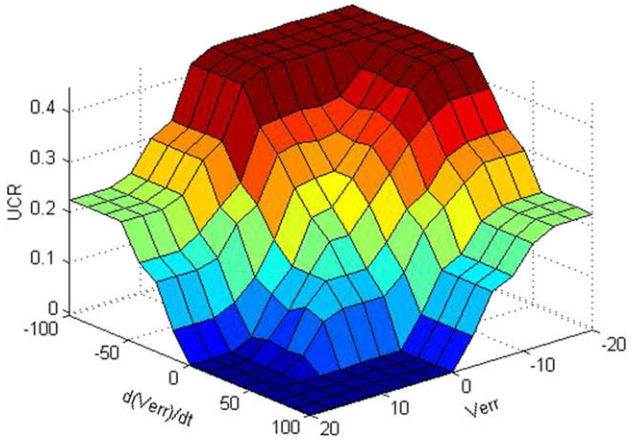

Fig. 8 – Fuzzy logic controller surface for UCR.

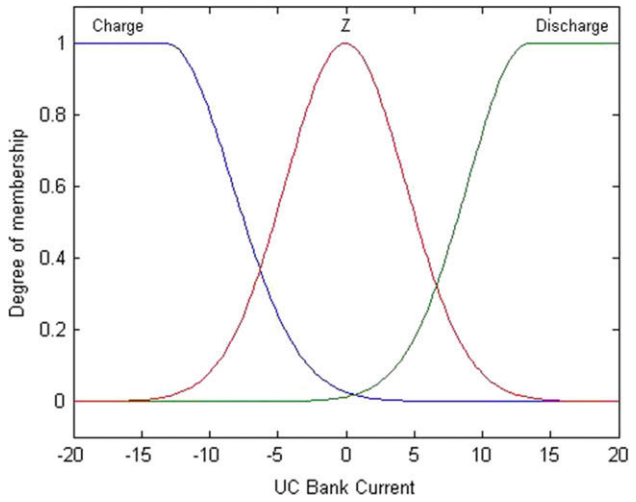

Fig. 9 – Membership function of the UC bank current.

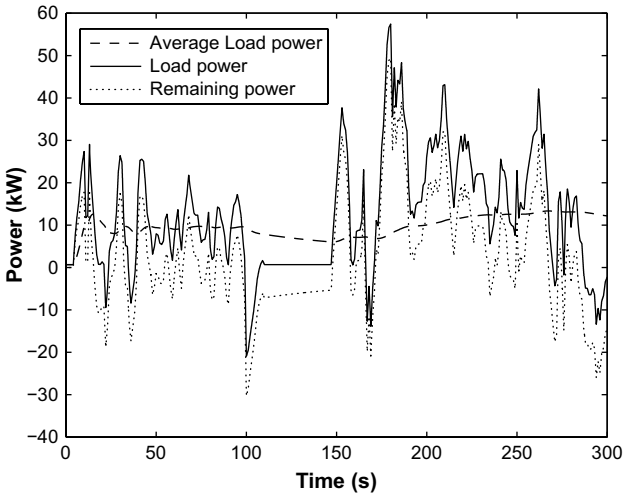

Fig. 10 – Proposed power sharing for the hybrid system components.

The calculation and optimization of the hybrid vehicle system size is a deliberate subject that requires a dedicated study by itself. In the literature, there are various studies using different calculation and optimization techniques for sizing energy sources [35–39]. Another method that is described in [40] is to use load filtering. In this method, steady -state load is extracted from the load profile using a filter averaged with a time constant of 20 s. Using this filter in the UDDS profile corresponds to a maximum power of 40 kW for the FC system. Based on these considerations, we chose our FC system to have 40 kW of rated power.

A second point to consider when sizing the FC system is its efficiency. In [39], using the same UDDS drive cycle, authors conclude that the maximum efficiency occurs at 40 kW rated FC system size. Moreover, among the fuel cell polarization curve, the most efficient operating interval for the fuel cell is the linear region corresponding to cell voltage between 0.55 and 0.8 V [5]. In our study, the cell voltage is sized at 0.8 V and the control strategy operates FC system such that cell voltage remains in this interval. The total stack voltage is $88 \times 0.8 = 70.4$ V which is the maximum operating voltage of the FC system. The minimum voltage is 50 V/88 = 0.57 V.

The entire UDDS can be divided into two regions based on the 20 s filter setting; low (<40 kW) and high (≥40 kW) power demand. The highest power demand for the cycle is 57.4 kW.

Table 2 – Rule base used for FC system output power.

ALC-I_{fc}	UC bank SOC				
	NM	NS	Z	PS	PM
NM	PM	PS	Z	NM	NM
NS	PM	PS	Z	NS	NM
Z	PM	PS	Z	NS	NM
PS	PM	PS	PS	Z	NS
PM	PM	PM	PM	PS	Z

Negative medium (NM), negative small (NS), zero (Z), positive small (PS), and positive medium (PM).

Therefore, a 40 kW FC system and a 20 kW UC bank are appropriate for our design. The base load power, supplied by FC system, ensures that the membrane is not subjected to sharp peak loads, thus increasing the lifetime of the FC system. Fuzzy logic control, described in Section 2.5, is used to make the decision on the power value to be delivered by the FC system.

Based on the load power profile and the FC system power rating, appropriate size of UC bank can be determined. About 75% of the initial energy stored in the UC bank can be used if the terminal voltage is allowed to decrease to 50% of its initial value [41]. The following parameters were used to start the UC bank design:

dt	Time of discharge	10 s
V_{max}	Maximum allowable terminal voltage	96 V
V_{min}	Minimum allowable terminal voltage	48 V
V_w	Operating terminal voltage	72 V
P	Power rating of the UC bank	20 kW

The total voltage drop dV_{total} of the UC bank is the sum of the voltage drops due to the capacitive and resistive components, expressed as [30]

$$dV_{total} = i_{avg} \cdot \frac{dt}{C} + i_{avg} \cdot R, \quad (18)$$

where i_{avg} is the average current of the UC bank [A], C is the capacitance [F], and R is the equivalent series resistance [Ω]. The allowable voltage drop in the proposed design may be expressed as

$$dV = V_w - V_{min} = 72 - 48 = 24V. \quad (19)$$

The average current to be supplied by the UC bank corresponds to the average of the maximum and minimum current demands from the UC bank i.e.,

Table 3 – Maxwell Boostcap BMOD0165 P048 ultracapacitor specifications [42].

Capacitance	165 F
Voltage	48.6 V
Dc resistance	6.1 mΩ
Ac resistance (@ 1 kHz)	5.2 mΩ
Weight	14.2 kg
Volume	12.6 L

$$i_{max} = \frac{P}{V_{min}} = \frac{20000}{48} = 416.6A, \quad (20)$$

$$i_{min} = \frac{P}{V_{max}} = \frac{20000}{96} = 208.3A, \quad (21)$$

$$i_{avg} = \frac{(416.6 + 208.3)}{2} = 312.5A. \quad (22)$$

For the proposed application, Maxwell Technologies Boostcap® BMOD0165 P048 type ultracapacitor bank is used. The specifications of the UC bank are given in Table 3.

In order to meet the power demand, four UC modules are used, where two strings of two modules connected in series. The total capacitance (C_{total}) and resistance (R_{total}) may be obtained as

$$C_{total} = C_{module} \bullet \frac{n_p}{n_s} = 165 \times \frac{2}{2} = 165F, \quad (23)$$

$$R_{total} = R_{module} \bullet \frac{n_s}{n_p} = 6.1 \times 10^{-3} \times \frac{2}{2} = 6.1m\Omega, \quad (24)$$

where n_p and n_s are the numbers of parallel and series connected capacitor modules, respectively.

Substituting the total capacitance and resistance values in Eq. (18) yields

$$dV = i \bullet \frac{dt}{C} + i \bullet R = 312.5 \times \frac{10}{165} + 312.5 \times 6.1 \times 10^{-3} = 20.8V. \quad (25)$$

Table 4 – FC system model parameters.

Activation voltage constant (B)	0.04777 (A^{-1})
Activation voltage constant (C)	0.0136 (V)
Faraday's constant (F)	96,484,600 (C (kmol)$^{-1}$)
Hydrogen time constant (τ_{H_2})	3.37 (s)
Hydrogen valve constant (K_{H_2})	4.22×10^{-5} (kmol (s atm)$^{-1}$)
Hydrogen–oxygen flow ratio (r_{H_2O})	1.168
K_r constant = No/4F	2.2802×10^{-7} (kmol (s A)$^{-1}$)
No load voltage (E_o)	0.8 (V)
Number of cells (N_o)	88
Number of fuel cell modules (N_s)	8
Oxygen time constant (τ_{O_2})	6.74 (s)
Oxygen valve constant (k_{O_2})	2.1×10^{-5} (kmol (s atm)$^{-1}$)
FC internal resistance (R_{int})	0.0303 (Ω)
FC absolute temperature (T)	343 (K)
Universal gas constant (R)	8314.47 (J (kmol K)$^{-1}$)
Utilization factor (U)	0.8
Water time constant (τ_{H_2O})	18.418 (s)
Water valve constant (K_{H_2O})	7.716×10^{-6} (kmol (s atm)$^{-1}$)

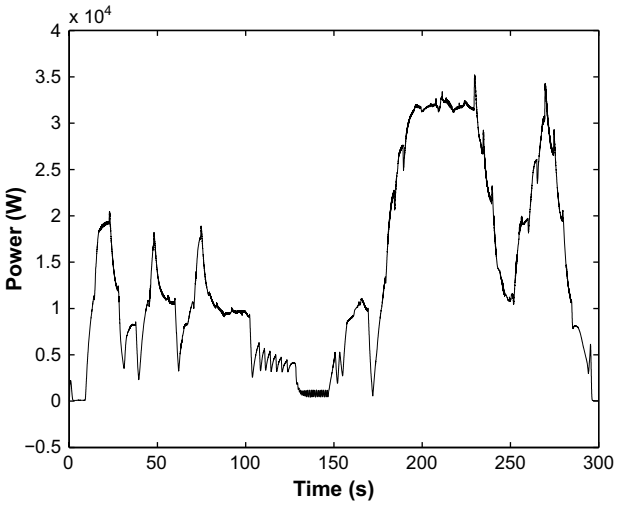

Fig. 11 – Dc–dc converter output power of the FC system.

Our original requirement allowed at most 24 V voltage change, and solution generated a voltage of 20.8 V. Therefore, it is evident that the proposed design is suitable for our application.

The PEMFC system parameters used in this research are shown in Table 4.

3. Simulation results

Simulation results are obtained by developing a detailed model using MATLAB, Simulink and SimPowerSystems using the mathematical and electrical models of the system described earlier. Simulations are conducted using a computer having 3 GB of RAM. Switching frequency of the power converters should be high, and therefore sample time could not exceed 50 μs for reliable operation. Moreover, since memory is limited, total simulation time was decreased to 300 s as shown in Fig. 10. Nevertheless, the highest power demand made by the vehicle is included in that time interval.

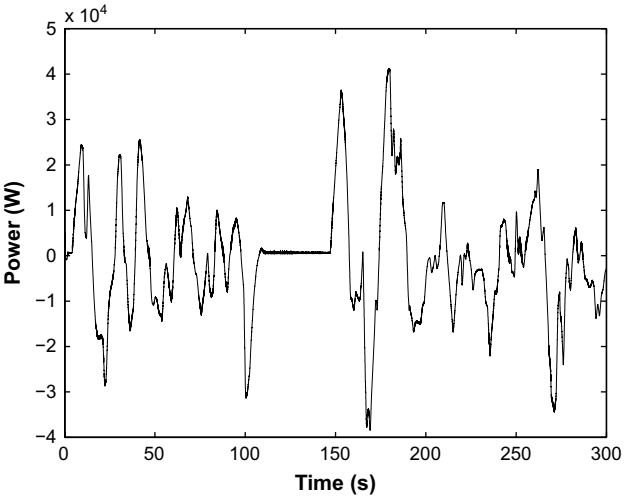

Fig. 12 – Dc–dc converter output power of the UC bank.

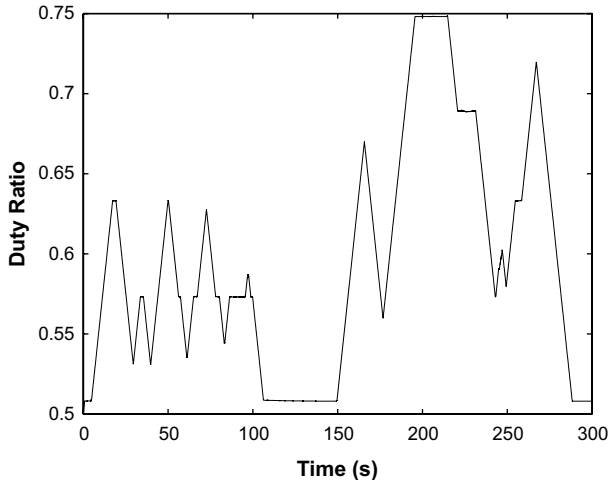

Fig. 13 – Dc–dc converter duty ratio of the FC system (FCR).

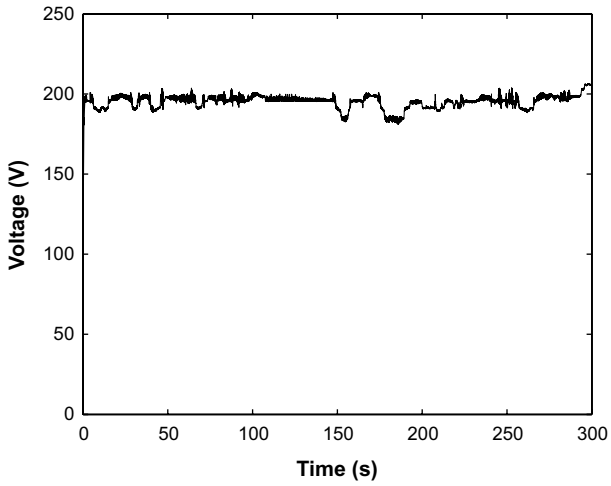

Fig. 15 – Load voltage.

Fig. 11 shows the power profile transmitted by the FC system to drive train. The FC system delivers the base power and it is slow in responding to sudden changes due to the internal dynamics even though it should follow the average load power. On the other hand, as illustrated in Fig. 12, during sudden changes in the load, the UC bank supplies peak power with alacrity. Its fast response fulfils the power demand and increases the hybrid system power density. It is also showed that compared to a battery, the ultracapacitor is capable enough to source and sink power in short durations. If a battery were used instead of the UC, the power profile showed in Fig. 12 would abuse the battery which may result in wear and reduced lifetime. In Fig. 13, FCR changes with respect to system dynamics and it is evident that FLC is capable of controlling the FC system output power by safely operating the UC bank. The FLC generates FCR to keep SOC between 0.5 and 0.95 when there is too much power need and power regeneration. Figs. 11 and 14 illustrate that in normal conditions where SOC is close to 0.75, the FC system produces the average load power and it does not respond to power peaks exceeding the average value of the load power unless the UC bank is in need of charge. On the other hand, the UC

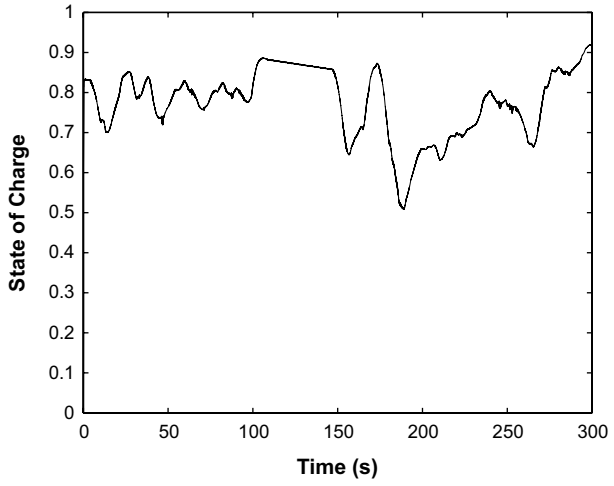

Fig. 14 – State-of-charge of the UC bank.

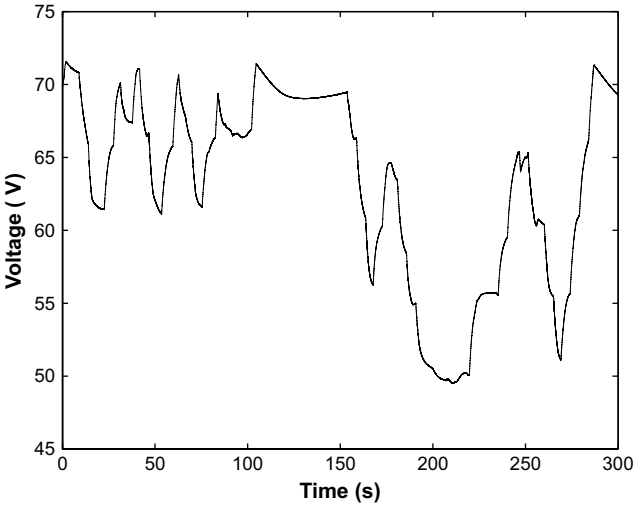

Fig. 16 – FC system output voltage.

bank supplies the peak power when it has enough charge and keeps the voltage within the allowable limits as shown in Fig. 15. Also, Fig. 15 shows that the dc bus voltage stays between 206 and 180 V thus satisfying a stable interval (±%10 for 188 V nominal dc bus voltage). Therefore, the hybrid system is capable of supplying enough power without fully relying upon the FC system which reduces the size and cost of the FC system. From Fig. 16, it is evident that the increase in load power decreases the FC output voltage according to the model dynamics. Even though the FC output voltage falls down to 50 V due to the high boosting ratio of the dc–dc converter, it is possible to deliver enough power to the high voltage dc bus.

4. Conclusions

A novel vehicular FC/UC hybrid power system is proposed using the fuzzy logic control strategy. The hybrid vehicular power system uses a novel control algorithm to meet the

power demand under various load conditions of the UDDS cycle. The proposed load sharing principle demands stable power supply from the FC system and effectively uses the UC bank for increasing the overall power capability of the hybrid system and regenerating the excess power during vehicle deceleration. The load power is partitioned so that the FC system delivers base load power and UC bank supplies the remaining power or regenerates the excess power.

While the FC system delivers stable power and keeps SOC at acceptable limits, the UC bank maintains load bus voltage within a tolerable range. The UC bank meets the peak power demanded by the drive train without drawing excessive current from the FC system yielding higher output power with lower cost. Also, it recuperates the braking energy as allowed by the FCR thus guaranteeing the operation of the UC bank within a tolerable region. The FLC effectively satisfies the power demand and manages efficient operation of the overall system.

The proposed hybrid power system combined with the new fuzzy logic control algorithm reduces the FC system size while satisfying the peak power demand via the UC bank. Thus, fuel consumption is decreased and the FC system is not exposed to insufficient humidification with gas starvation or flooding problems.

Acknowledgement

This work was supported in part by the U.S. Department of Energy under Grant DE-FG02-05CH11295.

REFERENCES

[1] Granovskii M, Dincer I, Marc AR. Life cycle assessment of hydrogen fuel cell and gasoline vehicles. Int J Hydrogen Energy 2006;31(3):337–52.
[2] Richard SP, Whale M, Djilali N. A techno-economic analysis of decentralized electrolytic hydrogen production for fuel cell vehicles. Int J Hydrogen Energy 2005;30(11):1159–79.
[3] Schlecht L. Competition and alliances in fuel cell power train development. Int J Hydrogen Energy 2003;28(7):717–23.
[4] Hauer K-H. Analysis tool for fuel cell vehicle hardware and software (controls) with an application to fuel economy comparisons of alternative system designs, Ph.D. dissertation, Dept. Transportation Technology and Policy, Univ. California, Davis; 2001.
[5] Barbir F. PEM fuel cells: theory and practice. Burlington, MA: Elsevier Academic Press; 2005. pp. 1-10, 342-344.
[6] Uzunoglu M, Alam MS. Dynamic modeling, design and simulation of a PEM fuel cell/ultracapacitor hybrid system for vehicular applications. Energy Conversion Manage 2007; 48(5):1544–53.
[7] Barbir F, Gomez T. Efficiency and economics of proton exchange membrane (PEM) fuel cells. Int J Hydrogen Energy 1997;22(10-11):1027–37.
[8] Corbo P, Migliardini F, Veneri O. Performance investigation of 2.4 kW PEM fuel cell stack in vehicles. Int J Hydrogen Energy 2007;32(18):4340–9.
[9] Haitao Y, Yulan Z, Zechang S, Gang W. Model-based power control strategy development of a fuel cell hybrid vehicle. J Power Sources 2008;180:821–9.
[10] Corbo P, Migliardini F, Veneri O. PEFC stacks as power sources for hybrid propulsion systems, Int J Hydrogen Energy, in press, doi:10.1016/j.ijhydene.2008.07.049.
[11] Sapienza C, Andaloro L, Matera FV, Dispenza G, Creti P, Ferraro M, et al. Batteries analysis for FC-hybrid powertrain optimization. Int J Hydrogen Energy 2008;33:3230–4.
[12] Thounthong P, Rael S, Davat B. Control strategy of fuel cell/supercapacitors hybrid power sources for electric vehicle. J Power Sources 2006;158:806–14.
[13] Rodatz P, Paganelli G, Sciarretta A, Guzzella L. Optimal power management of an experimental fuel cell/supercapacitor-powered hybrid vehicle. Control Eng Practice 2005;13:41–53.
[14] Burke A. Ultracapacitors: why, how, and where is the technology. J Power Sources 2000;91(1):37–50.
[15] Duran-Gomez JL, Enjeti PN, Von Jouanne A. An approach to achieve ride-through of an adjustable-speed drive with flyback converter modules powered by super capacitors. IEEE Trans Ind Appl 2002;38(2):514–22.
[16] Key TS, Sitzlar HE, Geist TD. Fast response, load-matching hybrid fuel cell, Final Technical Progress Report, EPRI PEAC Corp., Knoxville, Tennessee, NREL/SR-560-32743; 2003.
[17] Husain I. Electric and hybrid electric vehicles: design fundamentals. New York: CRC Press; 2003. pp. 88-92.
[18] Honda fuel cell power FCX [Online]. Available: http://world.honda.com/FuelCell/FCX/FCXPK.pdf, Press Information, 2004.12, accessed January 2008.
[19] Uzunoglu M, Alam MS. Modeling and analysis of an FC/UC hybrid vehicular power system using a novel wavelet based load sharing algorithm. IEEE Trans Energy Conversion 2008; 23(1):263–72.
[20] Dietrich P, Buchi F, Tsukada A, Bärtschi M, Kötz R, Scherer GG, et al. Hy. Power – a technology platform combining a fuel cell system and a supercapacitor. In: Vielstich W, Lamm A, Gasteiger HA, editors. Handbook of fuel cells – fundamentals, technology and application, vol. 4. New York: John Wiley&Sons Inc.; 2003. p. 1184–98.
[21] Choi D-K, Lee B-K, Choi S-W, Won C-Y, Yoo D-W. A novel power conversion circuit for cost-effective battery-fuel cell hybrid systems. J Power Sources 2005;152:245–55.
[22] Padulles J, Ault GW, McDonald JR. An integrated SOFC plant dynamic model for power systems simulation. J Power Sources 2000;86:495–500.
[23] El-Sharkh MY, Rahman A, Alam MS, Byrne PC, Sakla AA, Thomas T. A dynamic model for a stand-alone PEM fuel cell power plant for residential applications. J Power Sources 2004;138(1-2):199–204.
[24] Amphlett JC, Mann RF, Peppley BA, Roberge PR, Rodrigues A. A model predicting transient response of proton exchange membrane fuel cells. J Power Sources 1996;61:183–8.
[25] Hamelin J, Agbossou K, Laperriere A, Laurencelle F, Bose TK. Dynamic behavior of a PEM fuel cell stack for stationary applications. Int J Hydrogen Energy 2001;26:625–9.
[26] Amrhein M, Krein PT. Dynamic simulation for analysis of hybrid electric vehicle system and subsystem interactions, including power electronics. IEEE Trans Vehicular Technol 2005;54(3):825–36.
[27] Nelms RM, Cahela DR, Tatarchuk BJ. Modeling double-layer capacitor behavior using ladder circuits. IEEE Trans Aerosp Electron Syst 2003;39(2):430–8.
[28] Spyker RL, Nelms RM. Analysis of double-layer capacitors supplying constant power loads. IEEE Trans Aerosp Electron Syst 2000;36(4):1439–43.
[29] Spyker RL, Nelms RM. Classical equivalent circuit parameters for a double-layer capacitor. IEEE Trans Aerosp Electron Syst 2000;36(3):829–36.
[30] How to Determine the Appropriate Size Ultracapacitor for Your Application [Online]. Available: http://www.maxwell.

com/pdf/uc/General_Sizing-1007236.pdf, accessed January 2008.
[31] EPA Urban Dynamometer Driving Schedule (UDDS) [online]. Available: http://www.epa.gov/otaq/emisslab/methods/uddsdds.gif, accessed January 2008.
[32] Srinivasan S. Fuel cells: from fundamentals to applications. New York: Springer Science+Business Media; 2006. p. 180.
[33] Gao L, Dougal RA, Liu S. Power enhancement of an actively controlled battery/ultracapacitor hybrid. IEEE Trans Power Electron 2005;20(1):236–43.
[34] Xu H, Kong L, Wen X. Fuel cell power system and high power dc/dc converter. IEEE Trans Power Electron 2004;19(5):1250–5.
[35] Mellit A, Kolagirou SA, Hontoria L, Shaari S. Artificial intelligence techniques for sizing photovoltaic systems: a review. Renew Sustain Energy Rev. in press, doi:10.1016/j.rser.2008.01.006.
[36] Yang H, Zhou W, Lu L, Fang Z. Optimal sizing method for stand-alone hybrid solar-wind system with LPSP technology by using genetic algorithm. Solar Energy 2008;82:354–67.
[37] Kim M-J, Peng H. Power management and design optimization of fuel cell/battery hybrid vehicles. J Power Sources 2007;165:819–32.
[38] Lagorse J, Paire D, Miraoui A. Sizing optimization of a stand-alone street lighting system powered by a hybrid system using fuel cell, PV and battery. Renewable Energy 2009;34:683–91.
[39] Kim M, Sohn Y-J, Lee W-Y, Kim C-S. Fuzzy control based engine sizing optimization for a fuel cell/battery hybrid minibus. J Power Sources 2008;178:706–10.
[40] Zolot M. Dual-source energy storage – control and performance advantages in advanced vehicles. Long Beach, USA: The Electric Vehicle Symposium; 2003.
[41] Uzunoglu M, Alam MS. Dynamic modeling, design and simulation of a combined PEM fuel cell and Ultracapacitor system for stand alone applications. IEEE Trans Energy Conversion 2006;21(3):767–75.
[42] Maxwell Technologies BMOD0165-48.6V [Online]. http://www.maxwell.com/pdf/uc/datasheets/mc_power_series_48_1009365_rev3.pdf.
[43] Bose BK. Fuzzy logic and neural networks in power electronics and drives. IEEE Ind Appl Mag 2000;6(3):57–63.
[44] Mac-Vicar Whelan PJ. Fuzzy sets for man-machine interaction. Int J Man-Mach Studies 1976;8:687–97.